

# Thermodynamic Properties of Strongly Interacting Matter in Finite Volume using Polyakov-Nambu-Jona-Lasinio model

Abhijit Bhattacharyya\*

*Department of Physics, University of Calcutta, 92, A. P. C. Road, Kolkata - 700009, INDIA*

Paramita Deb†

*Theory Division, Physical Research Laboratory, Navarangpura, Ahmedabad - 380009, INDIA*

Sanjay K. Ghosh‡ and Rajarshi Ray§

*Department of Physics and Centre for Astroparticle Physics & Space Science,  
Bose Institute, 93/1, A. P. C Road, Kolkata - 700009, INDIA*

Subrata Sur¶

*Department of Physics, Panihati Mahavidyalaya,  
Barasat Road, Sodepur, Kolkata - 700110, INDIA*

We present the thermodynamic properties of strongly interacting matter in finite volume in the framework of Polyakov loop enhanced Nambu–Jona-lasinio model within mean field approximation. We considered both the 2 flavor and 2+1 flavor matter. Our primary observation was a qualitative change in the phase transition properties that resulted in the lowering of the temperature corresponding to the critical end point. This would make it favorable for detection in heavy-ion experiments that intend to create high density matter with considerably small temperatures. We further demonstrate the possibility of obtaining chiral symmetry restoration even within the confined phase in finite volumes.

PACS numbers: 12.38.Aw, 12.38.Mh, 12.39.-x

## I. INTRODUCTION

The strongly interacting matter is supposed to have a rich phase structure at finite temperatures and densities [1]. While our Universe at the present epoch contains a significant fraction of color singlet hadrons, color non-singlet states especially quarks and gluons may have been prevalent in the past – a few microseconds after the Big Bang [2]. The temperature of the Universe at that epoch is estimated to be  $\sim 200$  MeV. Similar state of matter is also expected to exist inside the core of super-massive stars in the present day Universe, where the density is  $\sim 10$  times that of normal nuclear matter. A direct study of such natural phenomenon is out of bounds even to modern astrophysicists. Fortunately experimental facilities at CERN (France/Switzerland), BNL (USA) and recently at GSI (Germany) are exploring the possibilities of creating and studying the properties of such exotic states of matter in a controlled environment. The key differences that appear in such experiments as compared to the natural phenomenon are the lifetime of matter created in the exotic state and its volume. Whereas in natural phenomenon the lifetime of the exotic matter may be large compared to the interaction time-scale, it is usually very small in an experimental situation. Some effects of the enhanced lifetime on the physical aspects of the system relating to the onset of equilibrium of weak interactions were discussed by us in Ref. [3]. Here we shall discuss about the effects of finite volume on the properties of strongly interacting matter.

In the following we shall generically define the matter with color confined states as the hadronic phase and the exotic state with colored degrees of freedom as the quark-gluon plasma (QGP). In the experiments this exotic phase may be produced by ultra relativistic collisions of heavy ions. The volume of the system thus created would depend on the nature of the colliding nuclei, the center of mass energy ( $\sqrt{s}$ ) and the centrality of collision. Once created, the system expands until the constituents are so far separated that their interaction ceases and they flow out as free streaming

---

\*Electronic address: abphy@caluniv.ac.in

†Electronic address: paramita.deb83@gmail.com

‡Electronic address: sanjay@bosemain.boseinst.ac.in

§Electronic address: rajarshi@bosemain.boseinst.ac.in

¶Electronic address: ssur.phys@gmail.com

particles. The distribution of particles thus freezes out, except for some further decays to smaller particles. There have been a large number of efforts to estimate the system size at freeze-out for different  $\sqrt{s}$  and different centralities. The most popular way of doing so is to measure the HBT radii. In Ref. [4] it has been shown that the freeze out volume increases as the  $\sqrt{s}$  increases. Here the authors have estimated the freeze out volume and found it to vary from  $2000 \text{ fm}^3$  to  $3000 \text{ fm}^3$ . In a very recent paper [5] the volume of homogeneity has been calculated using UrQMD model [6] and compared with the experimentally available results. The  $\sqrt{s}$  considered was in the range of 62.4 GeV to 2760 GeV for lead-lead collisions at different centralities. The system volume has been found to vary from  $50 \text{ fm}^3$  to  $250 \text{ fm}^3$ . Given that these are the freeze-out volumes, one can trace back to the initial equilibration time and expect an even smaller system size. In fact one cannot even consider the whole fireball, which is an isolated system to be in thermodynamic equilibrium. One has to choose a proper rapidity interval to act as the system under consideration. Therefore it becomes important to study how the various thermodynamic quantities in a strongly interacting matter depend on the volume of the system. Specifically we know that finite system sizes would lead to smoothening of any singularities appearing at a phase transition [7]. Thus important signatures of such transitions must be reanalyzed with the help of finite size scaling analysis [8]. In the context of heavy ion collisions such a possible analysis has been discussed in the literature (see e.g. [9–11]).

On the theoretical side a study of finite volume effects was done in Ref. [12] with a bag of non-interacting quarks and gluons and it was found that the effective degrees of freedom are reduced. In Ref. [13] a two model equation of state was used to show that the separation between the hadronic and QGP phases around the critical temperature loses its sharpness resulting in a soft effective equation of state. A few first principle study of pure gluon theory on space-time lattices were performed, showing the possibility of significant finite size effects [14, 15]. Similar studies are going on in various QCD inspired models. In Ref. [16, 17] the quark mass gap equation has been studied with Schwinger-Dyson equation parallel to equivalent Lattice QCD (LQCD) calculations and various meson properties are found to have significant volume dependence. There are studies with four-fermi type interactions in the NJL models [9, 18, 19], linear sigma models [10, 20, 21] and Gross-Neveu models [22]. While in Ref. [20] the scaling behavior of chiral phase transition for finite and infinite volumes has been studied, the character of phase diagram has been studied in Ref. [9, 10, 21, 22]. In refs. [18] and [19] the authors have studied the chiral properties as a function of the radius of a finite droplet of quark matter. The stability of such a droplet in the context of strangelet formation within the NJL model has been addressed in Ref. [23]. Size dependent effects of diquark states within 2-dimensional NJL model has been studied in Ref. [24] and that of magnetic field is discussed in Ref. [25].

In this work we shall use the Polyakov loop enhanced NJL (PNJL) model to study the thermodynamic properties of the strongly interacting matter in a finite volume. This model originated from the NJL model [26–29] which incorporates the global symmetries of QCD quite nicely. A four quark interaction term in the NJL Lagrangian is able to generate the physics of spontaneous breaking of chiral symmetry – a property of QCD which is manifested as the non-degenerate chiral partners of the low-mass hadrons. However a reasonable description of the physics of color confinement is missing. With the introduction of a background field in the NJL model, motivated by the dynamics of the Polyakov Loop [30], one obtains the PNJL model which describes a number of features of confinement physics quite satisfactorily (see e.g. [31–36]).

Certain aspects of finite volume effects in the PNJL model has been discussed in Ref. [37] through a coarse graining of the Lagrangian, followed by a Monte Carlo simulation. This method goes on similar lines as the numerical studies of LQCD. Normally this would involve the same kind of complex determinant problem that has plagued the direct LQCD computations for non-zero baryon number densities. So it may be desirable to keep using the saddle point approximation in PNJL model to study the finite volume effects. Here we make the first case study, albeit with some simplified assumptions towards that direction.

We organize our paper as follows. In the next section we briefly describe the PNJL model and the modifications for finite volume. In section III we describe phase transition at finite volume and in section IV we discuss the thermodynamic properties. The pion and sigma meson masses and the pion decay constant at finite volume have been discussed in section V. In section VI we summarize and conclude.

## II. THE PNJL MODEL

We shall consider the PNJL model with light flavors (2 flavor) and light plus strange flavors (2+1 flavor). In the PNJL model the gluon physics comes into play through the chiral point couplings between quarks (present in the NJL part) and a background field which represents Polyakov Loop dynamics. The Polyakov line is represented as,

$$L(\vec{x}) = \mathcal{P} \exp[i \int_0^\beta d\tau A_4(\vec{x}, \tau)] \quad (1)$$

where  $A_4 = iA_0$  is the temporal component of Euclidian gauge field  $(\bar{A}, A_4)$ ,  $\beta = \frac{1}{T}$ , and  $\mathcal{P}$  denotes path ordering.  $L(\bar{x})$  transforms as a field with charge one under global  $Z(3)$  symmetry. The Polyakov loop is then given by  $\Phi = (Tr_c L)/N_c$ , and its conjugate by,  $\bar{\Phi} = (Tr_c L^\dagger)/N_c$ . The gluon dynamics can be described as an effective theory of the Polyakov loops. The Polyakov loop potential can be expressed as,

$$\frac{\mathcal{U}'(\Phi[A], \bar{\Phi}[A], T)}{T^4} = \frac{\mathcal{U}(\Phi[A], \bar{\Phi}[A], T)}{T^4} - \kappa \ln(J[\Phi, \bar{\Phi}]) \quad (2)$$

where  $\mathcal{U}(\phi)$  is a Landau-Ginsburg type potential commensurate with the  $Z(3)$  global symmetry. Here we choose a form given in Ref. [32],

$$\frac{\mathcal{U}(\Phi, \bar{\Phi}, T)}{T^4} = -\frac{b_2(T)}{2}\bar{\Phi}\Phi - \frac{b_3}{6}(\Phi^3 + \bar{\Phi}^3) + \frac{b_4}{4}(\bar{\Phi}\Phi)^2, \quad (3)$$

where

$$b_2(T) = a_0 + a_1\left(\frac{T_0}{T}\right) + a_2\left(\frac{T_0}{T}\right)^2 + a_3\left(\frac{T_0}{T}\right)^3, \quad (4)$$

$b_3$  and  $b_4$  being constants. The second term in Eqn.(2) is the Vandermonde term which replicates the effect of  $SU(3)$  Haar measure and is given by,

$$J[\Phi, \bar{\Phi}] = (27/24\pi^2) \left[ 1 - 6\Phi\bar{\Phi} + 4(\Phi^3 + \bar{\Phi}^3) - 3(\Phi\bar{\Phi})^2 \right]$$

The corresponding parameters were earlier obtained in the above mentioned literature by choosing suitable values by fitting a few physical quantities as function of temperature obtained in LQCD computations. The set of values chosen here are,

$$a_0 = 6.75, a_1 = -1.95, a_2 = 2.625, a_3 = -7.44, b_3 = 0.75, b_4 = 7.5, \\ T_0 = 190 \text{ MeV}, \kappa = 0.2 \text{ (for 2 flavor)}, \kappa = 0.13 \text{ (for 2+1 flavor)}$$

For the quarks we shall use the usual form of the NJL model except for the substitution of a covariant derivative containing a background temporal gauge field. Thus the 2 flavor version of PNJL model is described by the Lagrangian,

$$\mathcal{L} = \sum_{f=u,d} \bar{\psi}_f \gamma_\mu i D^\mu \psi_f - \sum_f m_f \bar{\psi}_f \psi_f + \sum_f \mu_f \gamma_0 \bar{\psi}_f \psi_f \\ + \frac{g_S}{2} \sum_{a=1,2,3} [(\bar{\psi} \tau^a \psi)^2 + (\bar{\psi} i \gamma_5 \tau^a \psi)^2] - \mathcal{U}'(\Phi[A], \bar{\Phi}[A], T) \quad (5)$$

For 2+1 flavor the Lagrangian may be written as,

$$\mathcal{L} = \sum_{f=u,d,s} \bar{\psi}_f \gamma_\mu i D^\mu \psi_f - \sum_f m_f \bar{\psi}_f \psi_f + \sum_f \mu_f \gamma_0 \bar{\psi}_f \psi_f + \frac{g_S}{2} \sum_{a=0,\dots,8} [(\bar{\psi} \lambda^a \psi)^2 + (\bar{\psi} i \gamma_5 \lambda^a \psi)^2] \\ - g_D [\det \bar{\psi}_f P_L \psi_{f'} + \det \bar{\psi}_f P_R \psi_{f'}] - \mathcal{U}'(\Phi[A], \bar{\Phi}[A], T) \quad (6)$$

where  $f$  denotes the flavors  $u$  or  $d$  or  $s$  respectively. The matrices  $P_{L,R} = (1 \pm \gamma_5)/2$  are respectively the left-handed and right-handed chiral projectors, and the other terms have their usual meaning, described in details in refs. [33, 34, 36, 38–40]. This NJL part of the theory is analogous to the BCS theory of superconductor, where the pairing of two electrons leads to the condensation causing a gap in the energy spectrum. Similarly in the chiral limit, NJL model exhibits dynamical breaking of  $SU(N_f)_L \times SU(N_f)_R$  symmetry to  $SU(N_f)_V$  symmetry ( $N_f$  being the number of flavors). As a result the composite operators  $\bar{\psi}_f \psi_f$  pick up nonzero vacuum expectation values. The quark condensate is given as,

$$\langle \bar{\psi}_f \psi_f \rangle = -i N_c \mathcal{L} t_{y \rightarrow x} (tr S_f(x - y)), \quad (7)$$

where trace is over color and spin states. The self-consistent gap equation for the constituent quark masses are,

$$M_f = m_f - g_S \sigma_f + g_D \sigma_{f+1} \sigma_{f+2}, \quad (8)$$

where  $\sigma_f = \langle \bar{\psi}_f \psi_f \rangle$  denotes chiral condensate of the quark with flavor  $f$ . Here if we consider  $\sigma_f = \sigma_u$ , then  $\sigma_{f+1} = \sigma_d$  and  $\sigma_{f+2} = \sigma_s$ . Similarly if  $\sigma_f = \sigma_d$  then  $\sigma_{f+1} = \sigma_s$  and  $\sigma_{f+2} = \sigma_u$ , if  $\sigma_f = \sigma_s$  then  $\sigma_{f+1} = \sigma_u$  and  $\sigma_{f+2} = \sigma_d$ . The expression for  $\sigma_f$  at zero temperature ( $T = 0$ ) and chemical potential ( $\mu_f = 0$ ) may be written as [35],

$$\sigma_f = -\frac{3M_f}{\pi^2} \int^{\Lambda} \frac{p^2}{\sqrt{p^2 + M_f^2}} dp, \quad (9)$$

$\Lambda$  being the three-momentum cut-off. This cut-off have been used to regulate the model because it contains dimensional couplings rendering the model to be non-renormalizable.

Due to the dynamical breaking of chiral symmetry,  $N_f^2 - 1$  Goldstone bosons appear. These are the pions and kaons whose masses, decay widths etc. from experimental observations are utilized to fix the NJL model parameters. The parameter values have been listed in table I. Here we consider the  $\Phi$ ,  $\bar{\Phi}$  and  $\sigma_f$  fields in the mean field approximation (MFA) where the mean field are obtained by simultaneously solving the respective saddle point equations.

Model	$m_u$ MeV	$m_s$ MeV	$\Lambda$ MeV	$g_S \Lambda^2$	$g_D \Lambda^5$
2 flavor	5.5	0	651	4.27	0
2+1 flavor	5.5	134.76	631	3.67	9.33

TABLE I: Parameters of the Fermionic part of the model.

Now that the PNJL model is described for infinite volumes we discuss how we implement the finite volume constraints. Ideally one should choose the proper boundary conditions – periodic for bosons and anti-periodic for fermions. This would lead to a infinite sum over discrete momentum values  $p_i = \pi n_i / R$ , where  $i = x, y, z$  and  $n_i$  are all positive integers and  $R$  is the lateral size of a cubic volume. This implies a lower momentum cut-off  $p_{min} = \pi / R = \lambda$  (say). One should also incorporate proper effects of surface and curvatures. In this first case study we shall however take up a number of simplifications listed below:

- We shall neglect surface and curvature effects.
- The infinite sum will be considered as an integration over a continuous variation of momentum albeit with the lower cut-off.
- We shall not use any modifications to the mean-field parameters due to finite size effects. Thus the Polyakov loop potential as well as the mean-field part of the NJL model would remain unchanged. They shall feel the effect of changing volume only implicitly through the saddle point equations.

### III. PHASE TRANSITION

To study the finite volume effects on the thermodynamic properties of strongly interacting matter we begin by writing down the thermodynamic potential in MFA.

The expression is given by,

$$\begin{aligned} \Omega'(\Phi, \bar{\Phi}, \sigma_f, T, \mu_f) = & \mathcal{U}'[\Phi, \bar{\Phi}, T] + 2g_S \sum_{f=u,d,s} \sigma_f^2 - \frac{g_D}{2} \sigma_u \sigma_d \sigma_s \\ & - T \sum_n \int_{\lambda}^{\infty} \frac{d^3 p}{(2\pi)^3} Tr \ln \frac{S^{-1}(i\omega_n, \vec{p})}{T}. \end{aligned} \quad (10)$$

where  $\omega_n = \pi T(2n + 1)$  are Matsubara frequencies for fermions. The inverse quark propagator is given in momentum space by

$$S^{-1} = \gamma_0(p^0 + \hat{\mu} - iA_4) - \vec{\gamma} \cdot \vec{p} - \hat{M} \quad (11)$$

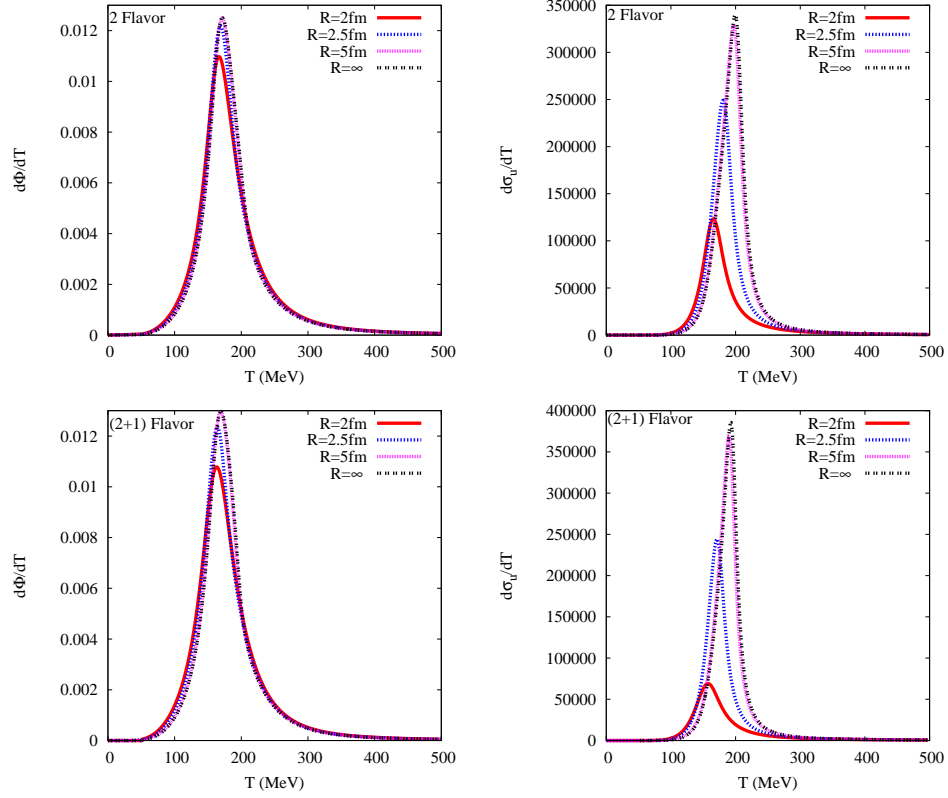


FIG. 1: (Color online) Derivatives of order parameters for chiral and deconfinement phase transition for different system sizes.

using the identity  $Tr \ln(X) = \ln \det(X)$ , we get,

$$\begin{aligned}
 \Omega' &= \mathcal{U}'[\Phi, \bar{\Phi}, T] + 2g_S \sum_{f=u,d,s} \sigma_f^2 - \frac{g_D}{2} \sigma_u \sigma_d \sigma_s - 6 \sum_f \int_{\lambda}^{\Lambda} \frac{d^3 p}{(2\pi)^3} E_{p_f} \Theta(\Lambda - |\vec{p}|) \\
 &- 2 \sum_f T \int_{\lambda}^{\infty} \frac{d^3 p}{(2\pi)^3} \ln \left[ 1 + 3(\Phi + \bar{\Phi} \exp(\frac{-(E_{p_f} - \mu_f)}{T})) \exp(\frac{-(E_{p_f} - \mu_f)}{T}) + \exp(\frac{-3(E_{p_f} - \mu_f)}{T}) \right] \\
 &- 2 \sum_f T \int_{\lambda}^{\infty} \frac{d^3 p}{(2\pi)^3} \ln \left[ 1 + 3(\bar{\Phi} + \Phi \exp(\frac{-(E_{p_f} + \mu_f)}{T})) \exp(\frac{-(E_{p_f} + \mu_f)}{T}) + \exp(\frac{-3(E_{p_f} + \mu_f)}{T}) \right] \\
 &= \Omega - \kappa T^4 \ln J[\Phi, \bar{\Phi}]
 \end{aligned} \tag{12}$$

where  $E_{p_f} = \sqrt{p^2 + M_f^2}$  is the single quasiparticle energy. In the last line  $\Omega$  contains all the terms of  $\Omega'$  except the Vandermonde term.

We now search for the saddle point of the thermodynamic potential which gives the temperature and density dependence of the fields. For all the system sizes, at zero baryon density, we found that the order parameters for both chiral ( $\sigma = \langle \bar{u}u \rangle + \langle \bar{d}d \rangle$ ) and deconfinement ( $\Phi$ ) transition smoothly passes from the hadronic phase to the quark phase. This indicates that the system does not have a real phase transition, rather there is a smooth crossover. The crossover temperature is identified to the point of inflection of  $\sigma_u$  and  $\Phi$  with temperature. In Fig. 1 we have plotted  $d\Phi/dT$  and  $d\sigma_u/dT$  for 2 flavor and 2+1 flavor matter for different system sizes. The peak position of these plots give respective inflection points. Note that, the deconfinement and chiral transitions do not take place exactly at the same temperature. Here we take the average of these two temperatures as  $T_c$ . The results are shown in table II, where we quote the different values of the crossover temperatures corresponding to different system sizes.

From table II it can be seen that the  $T_c$  has a strong dependence on system size. For 2 flavors the  $T_c$  varies from 167 MeV to 186 MeV which means a change of about 10%. A similar result is observed for 2+1 flavor. One should note that the shift in the  $T_c$  is mainly due to the shift in the transition temperature of the chiral phase transition. The transition temperature of the deconfining phase transition almost does not change. This result is similar to that

	$R = 2 \text{ fm}$	$R = 2.5 \text{ fm}$	$R = 3 \text{ fm}$	$R = 5 \text{ fm}$	$R = \infty$
$T_c \text{ (MeV) (2 flavor)}$	167	171	180	184	186
$T_c \text{ (MeV) (2+1 flavor)}$	160	167	174	180	181

TABLE II: Transition temperatures for different system sizes.

obtained with PNJL model on the lattice [37]. This is somewhat expected as the Polyakov loop potential feels the effect of changing volume only indirectly through the fields  $\Phi$  and  $\bar{\Phi}$ .

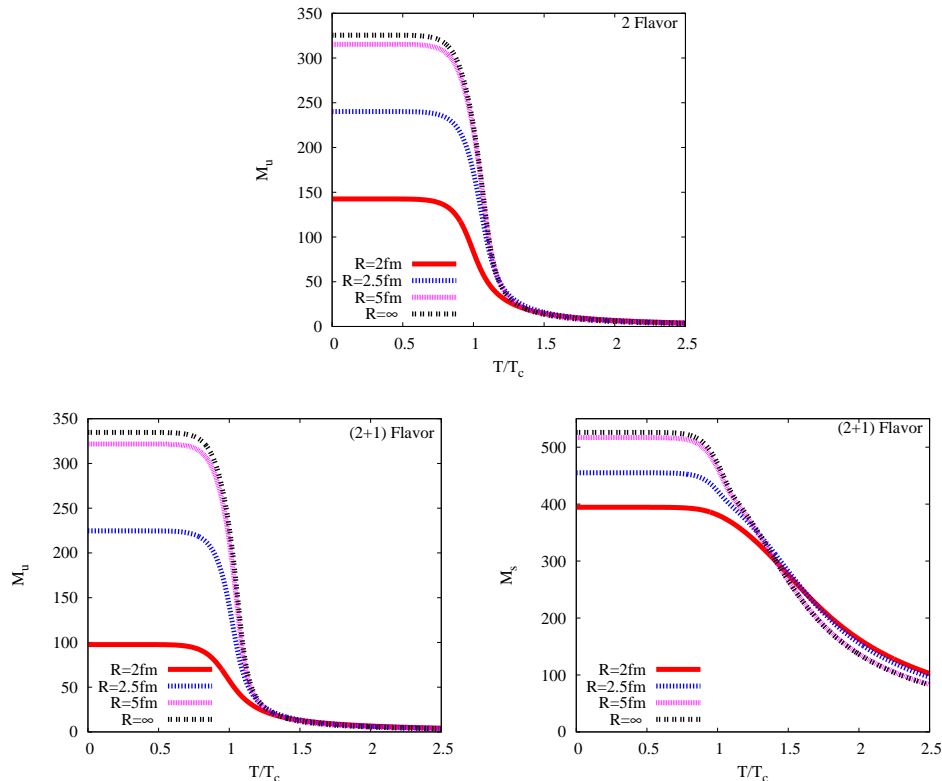


FIG. 2: (Color online) Constituent masses of quarks as a function of temperature for different system sizes.

In Fig. 2 we have plotted the temperature dependence of the constituent quark masses for both 2 flavors and 2+1 flavors. Below the crossover temperature they exhibit very strong volume dependence. Smaller the volume, smaller is the constituent mass. In the 2+1 flavor case, the masses of the light flavors drop faster than the strange quark. It thus seems that the chiral symmetry is gradually getting restored as one looks into smaller and smaller volumes. This is also the reason why the  $T_c$  itself is lowered for smaller volumes given in table II. Similar feature has also been observed in NJL models [18, 19]. Given that the quark condensation is similar to the superconducting condensate it is interesting to note that there are in fact certain superconductors which show similar decrease of band gap with the system size [41].

Let us now take a look into the situation at non-zero quark chemical potential  $\mu_q = \sum_f \mu_f / N_f$ . For infinite volume the phase transition is of first order and one observes a gap in the order parameter at sufficiently high chemical potential. At some smaller  $\mu_q$ , the first order transition ends at a critical end point (CEP). At this point the system undergoes a second order transition. At even smaller  $\mu_q$  we have only a crossover. As the volume of the system is lowered we find the phase transition characteristics fade away. Even the crossover characteristics start to die down. This is clear from the Fig. 3 where we plot  $d\sigma_u/dT$  and  $d\Phi/dT$  for  $\mu_q = 300 \text{ MeV}$  as a function of temperature. In Fig. 4 the phase diagram as a function of system size is shown. Note that the CEP gradually shifts towards higher  $\mu_q$  and lower  $T$  and finally disappears as the volume is reduced. This is an encouraging fact for the critical point search in heavy-ion collision experiments. To attain such high densities one needs to collide the ions at low  $\sqrt{s}$ , which means the temperature attained is lower. So if it were an infinite system one would have been far away from the CEP.

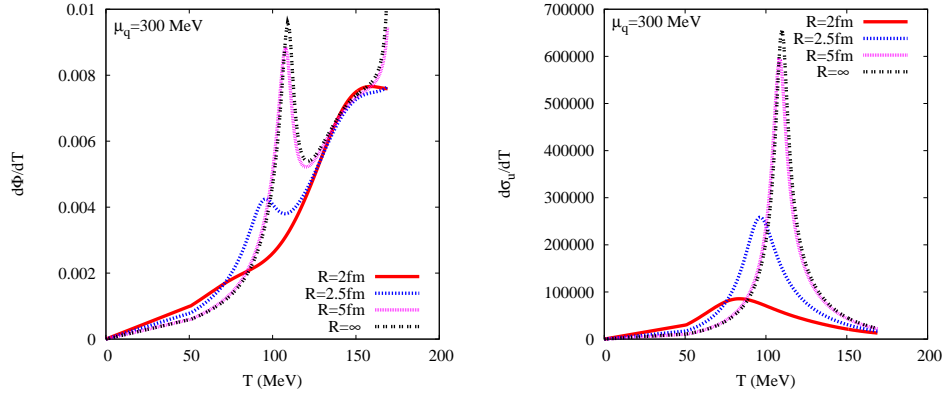


FIG. 3: (Color online) Derivatives of order parameters for chiral and deconfinement phase transition for 2 flavor at finite  $\mu_q$ .

Fortunately the experiments would produce small system volumes and this may lead to the location of the respective CEP possible. Thereafter one would need to do the finite size scaling analysis to extrapolate to the CEP for infinite volumes. The location of CEP for different volumes is collected in table III.

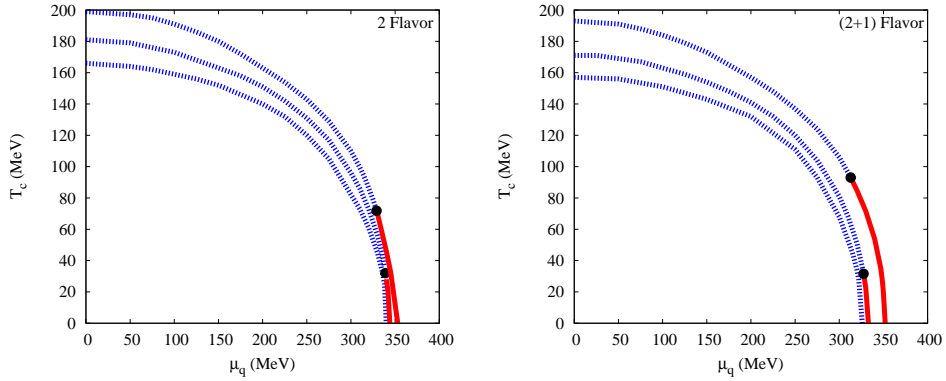


FIG. 4: (Color online) Phase diagram for different system sizes. The inside curve is for  $R = 2 \text{ fm}$ , the next curve is for  $R = 2.5 \text{ fm}$  and the outermost curve is for  $R = \infty$ .

	$R = 2 \text{ fm}$	$R = 2.5 \text{ fm}$	$R = 3 \text{ fm}$	$R = 5 \text{ fm}$	$R = \infty$
$T_c \text{ (MeV)}, \mu_{q_c} \text{ (MeV)}$ (2 flavor)	No CEP	32, 339	52, 335	69, 330	72, 329
$T_c \text{ (MeV)}, \mu_{q_c} \text{ (MeV)}$ (2+1 flavor)	No CEP	32, 328	60, 324	86, 316	93, 313

TABLE III: Location of chiral CEP for different system sizes.

#### IV. THERMODYNAMICS

In this section we discuss the behavior of a few thermodynamic observables namely pressure, energy density, specific heat, speed of sound etc. for different system sizes.

The pressure inside a volume  $V$  may be written as,  $P(T, \mu_q) = -\frac{\partial(\Omega(T, \mu_q)V)}{\partial V}$ , where  $T$  is the temperature and  $\mu_q$  is the quark chemical potential. In the top left panel of Fig. 5 we plot the temperature dependence of scaled pressure ( $P/T^4$ ) for 2 flavor system. As can be seen there is a significant change in scaled pressure for small system sizes. For example at  $T_c$  the  $P/T^4$  for a system with  $R = 2 \text{ fm}$  is almost half of that of an infinite system. As the temperature increases the difference slowly diminishes. The decrease of scaled pressure with increasing volume may be a surprise given that the constituent quark masses were shown to decrease drastically with decreasing volume, which should



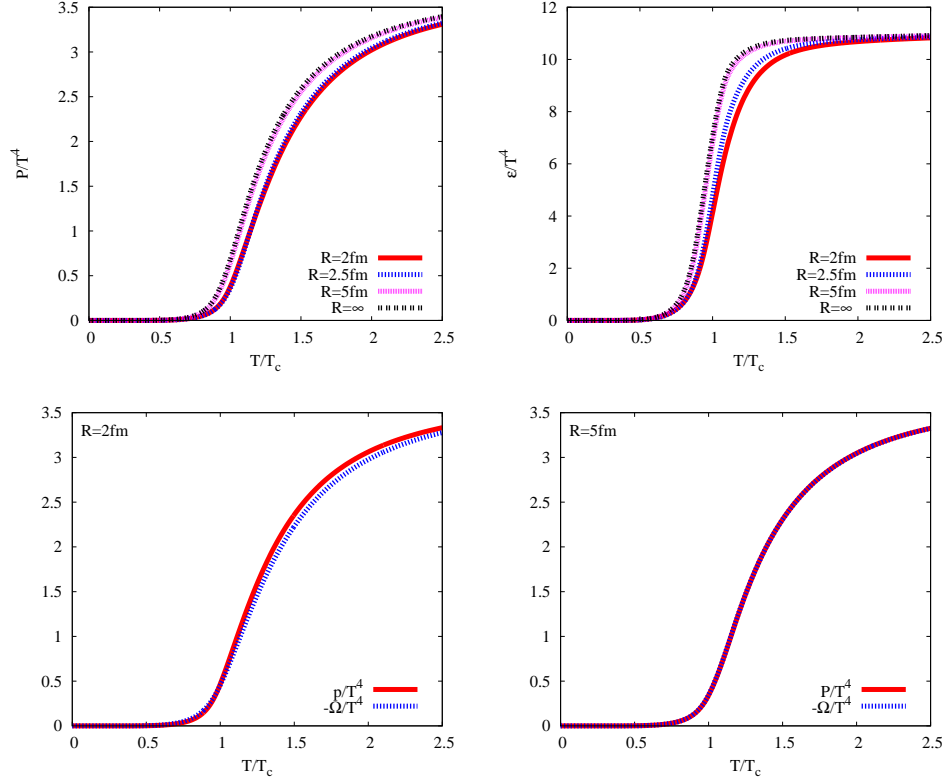


FIG. 5: (Color online) Pressure and energy density as a function of temperature (top panel). Comparison of pressure and  $-\Omega$ (bottom panel). These plots are for 2 flavor matter only.

imply increase in pressure. This can be understood as follows. With decreasing volume, not only the constituent masses decrease, but also the lowest momentum increases due to the infrared cut-off. These two conditions somehow seem to keep the lowest available energy of the quark quasi-particles almost same for different volumes. Thus the pressure does not increase with decreasing volume. However when plotted against  $T/T_c$  it seems to decrease because the  $T_c$  itself is smaller for smaller volumes, and therefore the pressure at the corresponding  $T/T_c$  for smaller volume is smaller than that for a larger volume.

The volume dependence is also quite strong for the energy density  $\epsilon = -T^2 \frac{\partial(\Omega/T)}{\partial T} \Big|_V = -T \frac{\partial \Omega}{\partial T} \Big|_V + \Omega$ . In the top right panel of the Fig. 5 we have plotted the  $\epsilon/T^4$  as a function of  $T/T_c$  for different system sizes. It has similar characteristics as  $P/T^4$  but the difference seems to diminish faster with increasing temperature. As the system size becomes  $R = 5\text{ fm}$  both the scaled pressure and scaled energy density converge to the  $R \rightarrow \infty$  case for almost all temperatures.

It is well known that for infinite volumes the definition of pressure simplifies to,  $P(T, \mu_q) = -\Omega(T, \mu_q)$ , which is commonly used the literature for PNJL models at infinite volumes. However since we are considering finite volumes here it would be interesting to check how much difference will it make if we keep using this definition rather than the correct one with a volume derivative. In the bottom two panels of Fig. 5 we have made a comparison of  $-\Omega/T^4$  and  $P/T^4$ . For  $R = 2\text{ fm}$  we see that these two quantities differ by about 10%. Again, as the size goes close to  $R = 5\text{ fm}$  this difference is almost washed out.

Let us now consider the quantity  $\epsilon - 3P$ . In our mean field approach this is the trace of the energy-momentum tensor given by,  $\mathcal{T}_{\mu\mu} = \epsilon - 3P$ . In a conformally symmetric theory, for example a theory of free massless quarks and gluons the energy momentum tensor is supposed to be zero as it signifies the conservation of the conformal currents. Thus  $\epsilon = 3P$  in that limit. In QCD however the conformal symmetry is broken due to non-zero quark masses as well as quantum anomalies as evident from the presence of a *scale* in the running coupling constant [42, 43]. Thus the energy-momentum tensor does not remain traceless. This was also found to be true in the PNJL model that have been reported in our earlier studies and compared with LQCD results [33, 38]. The PNJL model is however not QCD and the reason for the scale symmetry breaking is the introduction of an ultraviolet cut-off in the NJL part, a temperature scale  $T_0$  in the Polyakov loop part and of course a quark mass term similar to that in QCD. The



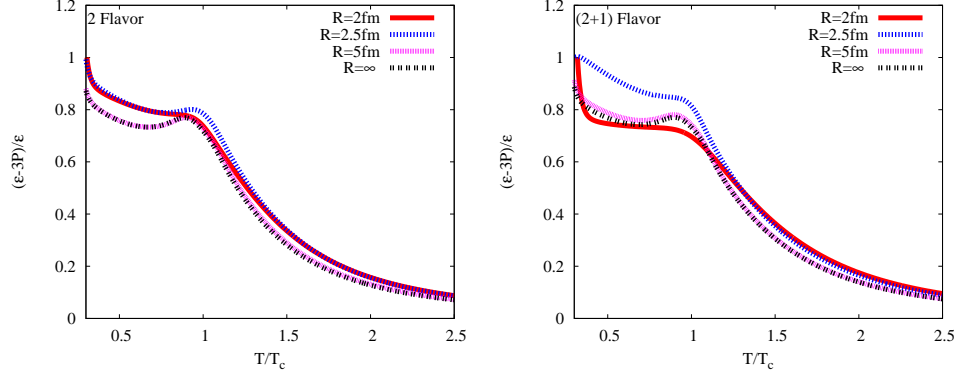


FIG. 6: (Color online) Conformal measure  $\mathcal{C} = 1 - 3P/\epsilon$  for different system sizes as a function of temperature.

physical implication of the two different scales in the quark and Polyakov sector is to give rise to separate crossover temperatures for the two sectors. To compare quantities obtained in PNJL model against LQCD results one then averages out two crossover temperatures as done by us here in the last section. Now for finite system sizes we have introduced an infrared cutoff which should further enhance the effect of conformal symmetry breaking. In fig. 6 we show the variation of the conformal measure  $\mathcal{C} = (\epsilon - 3P)/\epsilon$  with temperature for both 2 flavor and 2+1 flavor matter for different system sizes. That the smaller system sizes lead to larger conformal symmetry breaking effects is evident, except for the anomalous behavior of the lowest size of  $R = 2 \text{ fm}$ . (Though not shown in the figure we found that the anomalous behavior starts at a size between  $2 \text{ fm} \leq R \leq 2.5 \text{ fm}$ . The reason for this behavior is not clear at the moment and requires further investigation.)

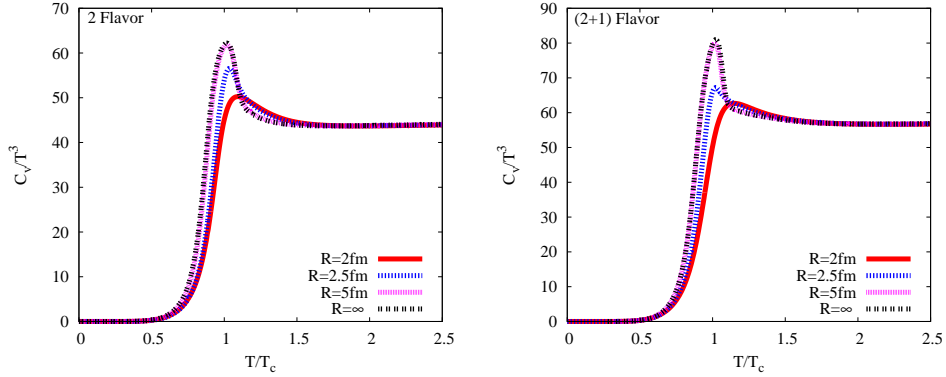


FIG. 7: (Color online) Variation of specific heat with temperature for different system sizes.

The specific heat at constant volume  $C_V = \left. \frac{\partial \epsilon}{\partial T} \right|_V$  is shown in Fig. 7. We find that with the change in volume,  $C_V$  changes prominently up to the temperature corresponding to the crossover region. For smaller volumes the specific heat is smaller indicating a higher rise in temperature for the same rise in energy density. Obviously this can be correlated with the temperature dependence of energy density discussed earlier in Fig. 5. We found that a given amount of scaled energy density is obtained at a higher scaled temperature for a smaller volume. This can be of interest in heavy-ion collision experiments. A given energy density deposited in the finite volume would create a plasma with temperature somewhat higher than that expected in a similar volume inside an infinite volume system having the same energy density.

The specific heat is also a measure of energy fluctuations in the system [44]. Fluctuations tend to rise sharply near a phase transition. For a crossover they are somewhat subdued. Obviously for finite volumes a true phase transition is not possible and as one keeps on decreasing the volume all signatures even for a crossover should die down. This is exactly the behavior of  $C_V$  as presented in Fig. 7.

The squared speed of sound  $v_s^2 = \frac{\partial P}{\partial \epsilon}$  is shown in Fig. 8. At large temperatures the  $v_s^2$  reaches its maximum value as the system becomes almost ideal. Interactions grow with decreasing temperatures resulting in the lowering of  $v_s^2$ .

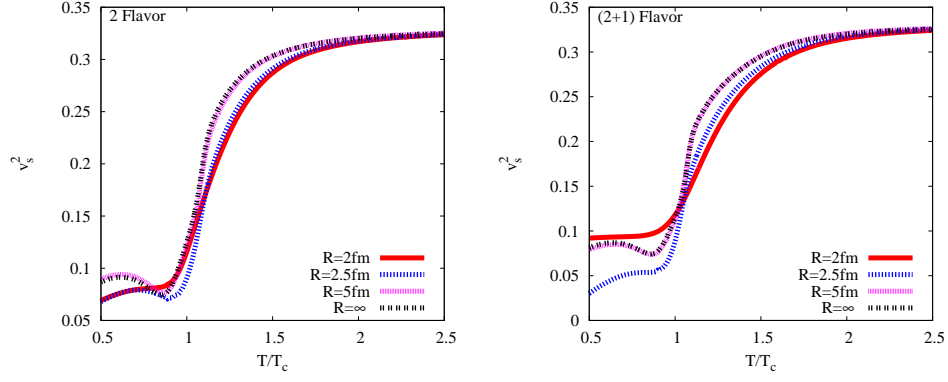


FIG. 8: (Color online) Variation of squared speed of sound with temperature for different system sizes.

The conformal measure  $\mathcal{C}$  may be considered as a measure of the strength of the interaction in the system. Thus lower the value of  $\mathcal{C}$ , higher should be the value of  $v_s^2$ . This is evident from Fig. 8, where we find the  $v_s^2$  to decrease with decreasing temperature, just opposite to the behavior of  $\mathcal{C}$  shown in Fig. 6. This correlation between  $\mathcal{C}$  and  $v_s^2$  also apparent for variation in volume. With decreasing volume the speed of sound decreases. (In fact an anomalous behavior for the smallest size  $R = 2 \text{ fm}$  is also apparent for  $v_s^2$ .) A smaller speed of sound for smaller volumes would mean a slower flow for finite size systems created in heavy-ion collisions.

## V. PROPERTIES OF NON-STRANGE MESONS

For infinite volumes the meson properties in the PNJL model has been discussed for 2 flavors [45] as well as for 2+1 flavors [36, 46]. In this section we describe the properties of non-strange mesons at finite volumes in the PNJL model. A detailed account of the calculational procedure for meson masses at finite temperatures and densities in the PNJL model may be found in Ref. [36]. Here we sketch the outline of the task.

The collective excitations, the fluctuation of the mean field around the vacuum can be handled within the Random Phase Approximation (RPA) [47]. In this approximation, which is equivalent to summing over the ring diagrams, the retarded correlation function for a meson  $M$  is given by,

$$C_M^> = \frac{\Pi^M}{1 - 2G_M\Pi^M}. \quad (13)$$

Here  $G_M$  is the suitable coupling constant and  $\Pi_M(k^2)$  is the one-loop polarization function for the mesonic channel under consideration. Within the RPA,  $\Pi^M$  may be written as,

$$\Pi^M \equiv \int_{\lambda}^{\Lambda} \frac{d^4p}{(2\pi)^4} \text{Tr} [\Gamma_M S(p+q) \Gamma_M S(q)], \quad (14)$$

where  $S(p)$  is the Hartree quark propagator,  $\Gamma_M$  is the appropriate combination of gamma matrices of different mesonic channels and the trace is taken over the Dirac and color spaces. The lower limit on the integration is now required for finite volume studies.

Here we concentrate on the scalar ( $\sigma$ ) and pseudoscalar ( $\pi$ ) channels. These contributions can be written as,

$$\begin{aligned} \Pi_{\pi}^{ab}(q^2) &= \int_{\lambda}^{\Lambda} \frac{d^4p}{(2\pi)^4} \text{Tr} (i\gamma_5 \tau^a S(p+q) i\gamma_5 \tau^b S(q)) \\ \Pi_{\sigma}(q^2) &= \int_{\lambda}^{\Lambda} \frac{d^4p}{(2\pi)^4} \text{Tr} (S(p+q) S(q)). \end{aligned} \quad (15)$$

The pole mass can be obtained by solving,

$$1 - 2G_M\Pi^M(\omega = m_M, \vec{q} = 0) = 0. \quad (16)$$

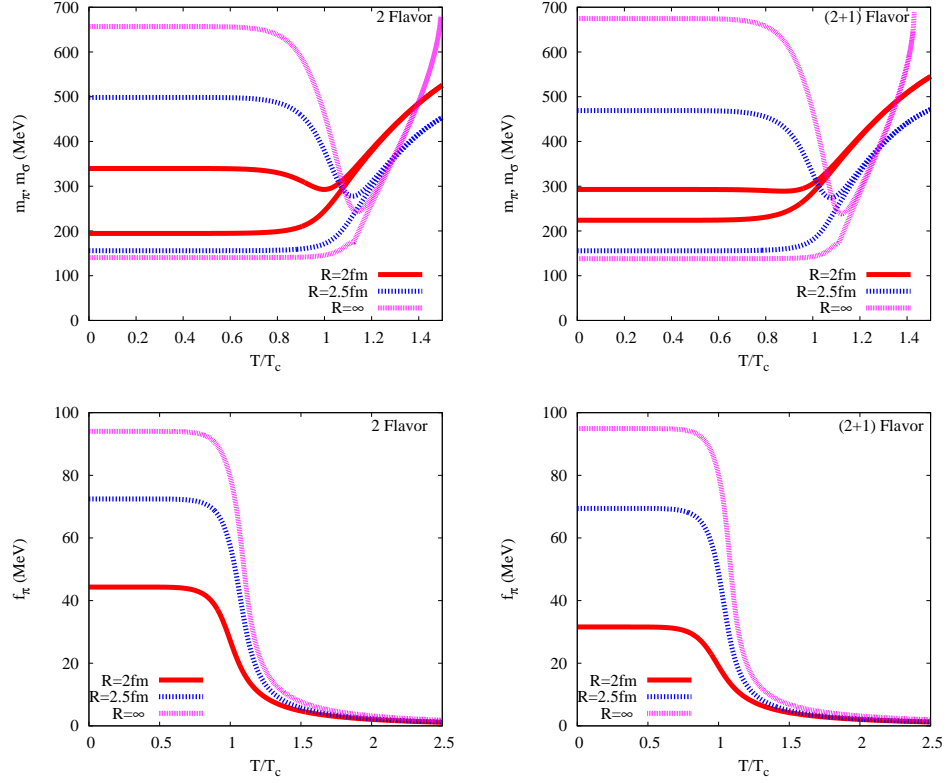


FIG. 9: (Color online) Variation of meson masses (upper panel) and pion decay constant (lower panel) with temperature for different system sizes. In the upper panel the three monotonously rising curves are for  $m_\pi$  and the other three are for  $m_\sigma$ .

where  $m_M$  is the mass of a particular meson. The detailed expression for  $\Pi^M$  and  $G_M$  for  $\pi$  and  $\sigma$  mesons may be found in Ref. [36].

In the upper panels of Fig. 9 we have plotted the masses of pion ( $m_\pi$ ) and sigma ( $m_\sigma$ ) as a function of temperature for different system sizes. In any given volume we see that for low temperatures the masses of pion and sigma are different and they become degenerate above  $T_c$  where chiral symmetry is expected to get restored. With decrease in volume we find the pion mass to increase. However above  $1.2 T_c$  the pion mass for infinite volume suddenly shoots up above those for the finite volumes. This may have important consequences in heavy-ion reactions where system size is small. Whereas for infinite volume the fast increasing mass of pion would drastically reduce chances of obtaining pion-like bound states, the same may not be true for finite volume.

While the mass of pion increases with decreasing volume at low temperatures the mass of sigma is found to decrease and that too quite fast. One can actually see a trend to the masses of the two chiral partners becoming closer to each other with decreasing volume. This, yet again, shows that chiral symmetry breaking effects reduce with decreasing volumes.

The pion decay constant may be obtained from the matrix element  $\langle 0 | J_{\mu,5}^a | \pi^b(k) \rangle = i \delta_{ab} f_\pi k_\mu$ , where  $J_{\mu,5}^a = \bar{\psi} \gamma_\mu \gamma_5 \frac{\tau^a}{2} \psi$  is the chiral current. At finite temperature and for a particular volume it can be written as (see [27, 28] and including the low momentum cut-off  $\lambda$ ),

$$f_\pi^2 = \frac{3M_u^2}{2\pi^2} \left[ \int_\lambda^\Lambda \frac{p^2 dp}{E_p^3} - 2 \int_\lambda^\infty \frac{p^2 dp}{E_p^3} f(E_p) \right] \quad (17)$$

where  $E_p = \sqrt{p^2 + M_u^2}$  is the single particle energy of a light quark and  $f(E_p)$  is the distribution function properly modified due to Polyakov loop interaction.

As shown in the lower panels of Fig. 9, the pion decay *constant* decreases both with the decrease in temperature and with that of system size. The decrease of  $f_\pi$  with temperature has also been observed in other effective models [45, 48], Dyson-Schwinger approaches [49] as well as in LQCD [50]. This is also an indication of the restoration of chiral symmetry as  $f_\pi$  is directly proportional to the divergence of the chiral current.

The tendency of chiral symmetry getting restored in finite volumes may also be noted by comparing Fig. 9 with Fig. 2. At low temperatures the constituent quark masses decrease with decreasing volume. It so happens that the light constituent quark masses become smaller than the pion mass for the smallest sizes studied here. These quarks should then become thermodynamically more favored than the pions. Though fortunately in the PNJL model, such constituent quarks will be suppressed due to the presence of the Polyakov loop, the pions would still lose their significance as the lightest particles that made them suitable candidates for becoming the Goldstone bosons. Thus what seems to happen is that the decrease of volume restores the spontaneous breaking of chiral symmetry in the same way as increase in temperature. The *critical size*  $R_c$  for such symmetry restoration would be somewhere between  $2\text{ fm}$  and  $2.5\text{ fm}$ . From Fig. 2 it may be noted that this range of sizes is almost equal to the respective constituent quark masses. This observation is commensurate with the expectation from chiral perturbation theory that chiral symmetry restoration may take place once the quark masses become equal to the inverse of system size [51].

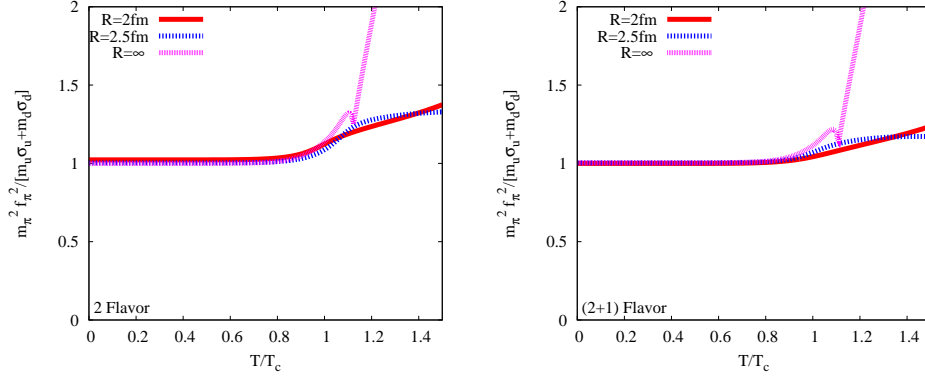


FIG. 10: (Color online) Checking for violation of the GMOR relation as a function of temperature and system size.

With all the strong indication of a possible chiral symmetry restoration with decreasing volume it would be interesting to see what happens to the Gell-Mann Oakes Renner (GMOR) [52] relation, which in the lowest order of chiral expansion is given by  $f_\pi^2 m_\pi^2 = m_u \sigma_u + m_d \sigma_d$ . Normally with increase in temperature as the spontaneously broken part of the chiral symmetry gets restored the GMOR relation should start to break down. This is exactly what we find in our calculations and shown in Fig. 10. But surprisingly we find that similar effect is not observed for the decrease in volume and the GMOR relation holds good for all the ranges of volumes we considered almost up to temperatures as high as  $0.8 T_c$ . In fact even at higher temperatures the GMOR relation is violated the most for infinite volumes. The way one can understand this is that for a physical chiral expansion a quantity  $m_\pi/\mathcal{M}$  is required, where  $\mathcal{M}$  is some suitable scale. In chiral perturbation theory  $\mathcal{M}$  is usually the nucleon mass, in zero temperature NJL or PNJL models it is the high momentum cut-off  $\Lambda$ , etc. For finite temperatures one can then consider  $T$  to play the role of  $\mathcal{M}$ . Thus, given a temperature if the corresponding  $m_\pi$  in a given volume is less than  $T$ , chiral identities would work properly (see e.g. [53]). So here we have a situation where chiral symmetry is getting restored while partial conservation of axial current is still maintained.

## VI. CONCLUSION

We have tried to understand the dynamics of strongly interacting matter inside finite volume in the framework of PNJL model with saddle point approximation. Several interesting results were observed that can have important implications for heavy-ion collision experiments. Our major finding was that the spontaneously broken chiral symmetry may be restored at much lower temperatures in small volume. This was shown through the computation of various thermodynamic observables as well as certain hadron properties.

Changes in the equation of state and speed of sound may have important consequences in the flow properties of the exotic medium created in the experiments. A measure of the specific heat in heavy-ion experiments is the transverse momentum fluctuations. We find the specific heat to decrease with decreasing volume indicating that the momentum fluctuations may not be as large as expected at a given  $T/T_c$ .

From the variation of the phase boundary with changing volume we demonstrated a stronger possibility of finding the signatures of a critical end point in low energy experiments that intend to create high baryonic densities where the expected temperature is not too high.

Finally from the hadron properties we observed the possibility of obtaining a chiral symmetric but confined phase in small volumes. We hope that a combination of heavy ion collisions and not-so-heavy ion collisions at similar center of mass energies, followed by an appropriate finite size scaling study may give us a better understanding of the QCD phase structure.

As discussed earlier we made a couple of simplified assumptions in this work. The Polyakov loop potential used here does not have an explicit volume dependence. The discrete momentum states in the quark potential was replaced with a continuum, and the only explicit dependence on system size was through the lower momentum cut-off. Though we believe that these assumptions would not affect the gross features observed, we hope to address these issues in future.

### Acknowledgments

We would like to thank Sanatan Dugal, Tamal K. Mukherjee and Ajit M. Srivastava for many useful discussions and comments. A.B. thanks UGC (UPE and DRS) and DST and R.R. thanks DST for support.

- 
- [1] K. Rajagopal and F. Wilczek, in 'At the frontier of particle physics / Handbook of QCD', M. Shifman (Ed.), World Scientific (Pub.) **3**, 2061 (2000) (arXiv:hep-ph/0011333).
  - [2] E. W. Kolb and M. S. Turner, in 'Frontiers in Physics : The Early Universe', D. Pines (Ed.), Perseus Books Group (Pub.) (1994).
  - [3] A. Bhattacharyya, S. K. Ghosh, S. Majumder and R. Ray, arXiv:1107.5941 (to be published).
  - [4] D. Adamova *et. al.*, Phys. Rev. Lett. **90**, 022301 (2003).
  - [5] G. Graef, M. Bleicher and Q. Li, Phys. Rev. C **85**, 044901 (2012).
  - [6] S. Bass *et. al.*, Prog. Part. Nucl. Phys. **41**, 225 (1998); M. Bleicher *et. al.*, J. Phys. G: Nucl. Part. Phys. **25**, 1859 (1999); H. Petersen, J. Steinheimer, G. Burau, M. Bleicher and H. Stöcker Phys. Rev. C **78**, 044901 (2008).
  - [7] M. E. Fisher and A. E. Ferdinand, Phys. Rev. Lett. **19**, 169 (1967).
  - [8] A. E. Ferdinand and M. E. Fisher, Phys. Rev. **185**, 832 (1969); M. E. Fisher and M. N. Barber, Phys. Rev. Lett. **28**, 1516 (1972). M. N. Barber, in 'Phase Transitions and Critical Phenomenon', C. Domb and J. L. Lebowitz (Eds.), Academic Press (Pub.), **8**, 146 (1987); J. L. Cardy, *Scaling and Renormalization in Statistical Physics*, (Cambridge, New York, 1996); D. Amit, *Field Theory; The Renormalization Group and Critical Phenomena*, (World Scientific, 2005).
  - [9] L. M. Abreu, M. Gomes and A. J. da Silva, Phys. Lett. B **642**, 551 (2006).
  - [10] L. F. Palhares, E. S. Fraga and T. Kodama, J. Phys. G **38**, 085101 (2011).
  - [11] E. S. Fraga, L. F. Palhares and P. Sorensen, Phys. Rev. C **84**, 011903(R) (2011).
  - [12] H.-T. Elze and W. Greiner, Phys. Lett. B **179**, 385 (1986).
  - [13] C. Spieles, H. Stoecker and C. Greiner, Phys. Rev. C **57**, 908 (1998).
  - [14] A. Gopie and M. C. Ogilvie, Phys. Rev. D, **59**, 034009 (1999).
  - [15] A. Bazavov and B. A. Berg, Phys. Rev. D **76**, 014502 (2007).
  - [16] C. S. Fischer and M. R. Pennington, Phys. Rev. D **73**, 034029 (2006).
  - [17] J. Luecker, C. S. Fischer and R. Williams, Phys. Rev. D **81**, 094005 (2010).
  - [18] O. Kiriya and A. Hosaka, Phys. Rev. D **67**, 085010 (2003).
  - [19] G. Shao, L. Chang, Y. Liu and X. Wang, Phys. Rev. D **73**, 076003 (2006).
  - [20] J. Braun, B. Klein and P. Piasecki, Eur. Phys. J. C **71**, 1576 (2011).
  - [21] J. Braun, B. Klein and B.-J. Schefer, Phys. Lett. B **713**, 216 (2012).
  - [22] F. C. Khanna, A. P. C. Malbouisson, J. M. C. Malbouisson and A. E. Santana, Eur. Phys. Lett. **97** 11002 (2012).
  - [23] S. Yasui and A. Hosaka, Phys. Rev. D **74**, 054036 (2006).
  - [24] L. M. Abreu, A. P. C. Malbouisson and J. M. C. Malbouisson, Phys. Rev. D **83**, 025001 (2011).
  - [25] L. M. Abreu, A. P. C. Malbouisson and J. M. C. Malbouisson, Phys. Rev. D **84**, 065036 (2011).
  - [26] Y. Nambu and G. Jona-Lasinio, Phys. Rev. **122**, 345 (1961), **124**, 246 (1961).
  - [27] S. P. Klevansky, Rev. Mod. Phys. **64** 649 (1992).
  - [28] T. Hatsuda and T. Kunihiro, Phys. Rept. **247**, 221 (1994).
  - [29] T. Kunihiro and T. Hatsuda, Phys. Lett. B **206**, 385 (1988).
  - [30] L. D. McLerran and B. Svetitsky, Phys. Rev. D **24**, 450 (1981); B. Svetitsky and L. G. Yaffe, Nucl. Phys. B **210**, 423 (1982); B. Svetitsky, Phys. Rept. **132**, 1 (1986). R. D. Pisarski, Phys. Rev. D **62** 111501 (2000); Marseille 2000, Strong and electroweak matter pg. 107-117 (hep-ph/0101168); E. Megias, E. Ruiz Arriola, L.L. Salcedo, Phys. Rev. D **69**, 116003 (2004); D. Diakonov and M. Oswald, Phys. Rev. D **70**, 105016 (2004); A. Dumitru and R. D. Pisarski, Phys. Lett. B **504**, 282 (2001); Phys. Rev. D **66**, 096003 (2002); Nucl. Phys. A **698**, 444 (2002); O. Scavenius, A. Dumitru and J. T. Lenaghan, Phys. Rev. C **66**, 034903 (2002).

- [31] K. Fukushima, Phys. Lett. B **591**, 277 (2004).
- [32] C. Ratti, M. A. Thaler and W. Weise, Phys. Rev. D **73**, 014019 (2006).
- [33] S. K. Ghosh, T. K. Mukherjee, M. G. Mustafa and R. Ray, Phys. Rev. D **73**, 114007 (2006); S. Mukherjee, M. G. Mustafa and R. Ray, Phys. Rev. D **75**, 094015 (2007).
- [34] S. K. Ghosh, T. K. Mukherjee, M. G. Mustafa and R. Ray, Phys. Rev. D **77**, 0904024 (2008).
- [35] M. Ciminale, R. Gatto, N. D. Ippolito, G. Nardulli and M. Ruggieri, Phys. Rev. D **77**, 054023 (2008).
- [36] P. Deb, A. Bhattacharyya, S. Datta and S. K. Ghosh, Phys. Rev. C **79**, 055208 (2009).
- [37] M. Cristoforetti, T. Hell, B. Klein and W. Weise, Phys. Rev. D **81**, 114017 (2010).
- [38] A. Bhattacharyya, P. Deb, S. K. Ghosh and R. Ray, Phys. Rev. D **82**, 014021 (2010).
- [39] A. Bhattacharyya, P. Deb, A. Lahiri and R. Ray, Phys. Rev. D **82**, 114028 (2010).
- [40] A. Bhattacharyya, P. Deb, A. Lahiri and R. Ray, Phys. Rev. D **83**, 014001 (2011).
- [41] S. Bose, P. Raychaudhuri, R. Banerjee, P. Vasa and P. Ayyub, Phys. Rev. Lett. **95** 147003 (2005).
- [42] J. C. Collins, A. Duncan and S. D. Joglekar, Phys. Rev. D **16**, 438 (1977).
- [43] N. K. Nielsen, Nucl. Phys. B **120**, 212 (1977).
- [44] R. Korus, St. Mrowczynski, M. Rybczynski and Z. Wlodarczyk, Phys. Rev. C **64**, 054908 (2001).
- [45] Wei-jie Fu and Yu-xin Liu, Phys. Rev. D **79**, 074011 (2009).
- [46] P. Costa, M. C. Ruivo, C. A. de Sousa, H. Hansen and W. M. Alberico, Phys. Rev. D **79**, 116003 (2009).
- [47] A. L. Fetter and J. D. Walecka, "Quantum Theory of Many-Particle System", McGraw-Hill, U. S. A. (1971).
- [48] A. Barducci, R. Casalbuoni, S. De Curtis, R. Gatto and G. Pettini, Phys. Lett. B **240**, 429 (1990); A. Barducci, R. Casalbuoni, S. De Curtis, R. Gatto and G. Pettini, Phys. Rev. D **42**, 1757 (1990); S. Jeon and J. Kapusta, Phys. Rev. D **54**, 6475 (1996); O. Kiriya,\*, M. Maruyama, and F. Takagi Phys. Rev. D **58**, 116001 (1998).
- [49] M. Harada and A. Shibata, Phys. Rev. D **59**, 014010 (1998); J. Luecker, C. S. Fischer and R. Williams, Phys. Rev. D **81**, 094005 (2010).
- [50] E. Laermann and F. Pucci, arXiv:1207.6615 (2012).
- [51] J. Gasser and H. Leutwyler, Nucl. Phys. B **307**, 763 (1988).
- [52] M. Gell-Mann, R. J. Oakes and B. Renner, Phys. Rev. **175**, 2195 (1968).
- [53] D. T. Son and M. A. Stephanov, Phys. Rev. D **66**, 076011 (2002).